Identification of Pumping Influences in Long-Term Water-Level Fluctuations

Dylan R. Harp dharp@lanl.gov

Velimir V. Vesselinov vvv@lanl.gov

Computational Earth Science Group

Earth and Environmental Sciences Division

Los Alamos National Laboratory

MS T003, Los Alamos, NM 87544, USA.

April 9, 2010

Abstract

Identification of the pumping influences at monitoring wells caused by spatially and temporally variable water-supply pumping can be a challenging, yet important hydrogeological task. The information that can be obtained can be critical for conceptualization of the hydrogeological conditions and indications of the zone of influence of the individual pumping wells. However, the pumping influences are often intermittent and small in magnitude with variable production rates from multiple pumping wells. While these difficulties may support an inclination to abandon the existing dataset and conduct a dedicated pumping test, that option can be challenging and expensive to coordinate and execute. This paper presents a method that utilizes a simple analytical modeling approach for analysis of a long-term water-level record utilizing an inverse modeling approach. The methodology allows the identification of pumping wells influencing the water-level fluctuations. Thus the analysis provides an efficient and cost-effective alternative to designed and coordinated multiple-well pumping tests. We apply this method on a dataset from the Los Alamos National Laboratory site. Our analysis also provides (1) an evaluation of the information content of the transient water-level data (to what extent the observed water-level transients are characterizing pumping influences), (2) indications of potential structures of the aquifer heterogeneity inhibiting or promoting pressure propagation, and (3) guidance for the development of more complicated models requiring detailed specification of the aquifer heterogeneity.

Introduction

Identification of the pumping influences at a monitoring well due to pumping at water-supply wells and respective estimation of the aquifer properties has traditionally been performed by analysis of a series of coordinated multiple-well pumping tests (i.e. coordinated events measuring the pressure influence at one or more monitoring wells while restricting pumping to a single pumping well; sometimes also referred to as cross-hole pumping tests). However, the planning and execution of these tests can be expensive and challenging. In many cases, it is logistically infeasible to cease water-supply pumping in the entire aquifer to conduct a dedicated pumping test (which includes pre- and post-pumping recovery periods) to eliminate influences from nearby water-supply wells. As advocated by *Yeh and Lee* (2007), existing datasets from monitoring well networks recorded during long-term pumping of water-supply wells provide an alternative to datasets generated by dedicated pumping test. Such datasets are frequently collected in monitoring-well networks established near contamination sites and municipal water-supply wells (*Barnett et al.*, 2003; *Gross*, 2007; *Mason et al.*, 2005; *Hix*, 2007; *Koch and Schmeer*, 2009). However, the pumping influences are often intermittent and small in magnitude compared with water level fluctuations caused by other hydrogeologic mechanisms (for example, recharge transients), causing the identification of the pumping influences due to a complex spatially and temporally variable water-supply pumping regime to be difficult.

The analysis may require the use of complicated computational models and involve large data sets that are challenging to process. Nevertheless, when compared to dedicated pumping tests, this approach provides some important advantages. First, the collected data are representative of the aquifer properties during existing water-supply conditions, while the aquifer properties obtained by pumping-test interpretations may need to be upscaled to be applied for simulation of the flow conditions under water-supply pumping. Second, the aquifer is typically stressed more intensively, due to the long-term pumping of multiple wells, with pressure influences affecting larger areas, providing better identification of pumping influences causing small water-level fluctuations. Third, the effect of measurement errors on the modeling effort can be minimized due to the large number of observations and by repeated pumping cycles often present in the long-term data record. Last, interpretation of transient water-level data at multiple monitoring wells influenced by transient pumping at multiple water-supply wells may provide information about the large-scale aquifer structures. Furthermore, the analyses can be extended to provide a tomographic characterization of aquifer properties (e.g. *Neuman* (1987); *Vesselinov et al.* (2001); *Straface et al.* (2007)). The identification of the pumping influences at the monitoring wells can also be critical for conceptualization of the hydrogeological conditions at the site, and provide indications of the extent of the zone of influence of the individual pumping wells.

Current trends in hydrogeology are focusing on data assimilation (*Vrugt et al.*, 2005; *Hendricks Franssen and Kinzelbach*, 2008) and geostatistical inverse approaches (*Certes and de Marsily*, 1991; *Gómez-Hernández et al.*, 1997; *Alcolea et al.*, 2006; *Harp et al.*, 2008) applied to distributed-parameter numerical models. These approaches possess the ability to consider details of heterogeneous aquifer properties, and are therefore attractive to researchers desiring a detailed representation of aquifer properties. It has been recognized that these approaches suffer from numerical instabilities, equifinality of solutions (*Beven*, 2000), low parameter sensitivities (*Carrera et al.*, 2005), and computational inefficiencies. While these approaches are typically successful in matching simulations to observations, it is often unclear whether this demonstrates a realistic representation of aquifer properties, or is merely a demonstration that a mathematical model with enough degrees of freedom can simulate a set of observations (*Beven*, 2006; *Grayson et al.*, 1992). Large efforts are underway to overcome the limitations of fitting distributed-parameter models, and their incisiveness will undoubtedly improve. This paper presents an alternative to the distributed model approach, using a minimally-parameterized analytical model. While this approach may be limited in its ability to represent heterogeneous aquifer properties, its benefits are computational efficiency and the ability to obtain incisive conclusions.

von Asmuth et al. (2008) demonstrates the decomposition of multiple stresses using minimally parameterized models in a time-series analysis framework. Our research is in line with their approach, however, our approach is developed directly from concepts of parameter estimation and inverse modeling, and therefore, may be more interpretable to modelers.

The decomposition of pressure influences requires a model with the ability to characterize the hydraulic response at a monitoring well due to transient pumping at the water-supply wells. Adequate characterization of the water-level transients requires calibration of the model in the form of parameter estimation. If the model is complicated with a large number of adjustable parameters, the calibration can become computationally demanding. As a result, the optimal parameter estimates may be difficult to identify and the parameter estimation may not have a unique solution (i.e. the inverse problem can become ill-posed) (*Carrera et al.*, 2005). To avoid this, we attempt to use the simplest possible model that can be satisfactorily applied. We choose to use analytical methods here for simulating pumping influences at the observation wells. The use of analytical methods makes the analysis consistent with pumping-test interpretations where analytical type-curve methods are commonly applied (*Freeze and Cherry*, 1979).

Theis (1935) introduced an analytical solution of the general equation for flow of a Newtonian fluid in porous media for non-steady conditions (Theis solution). The Theis solution is valid for simplified hydrogeologic scenarios assuming a constant pumping rate, horizontal flow, transmissivity and storativity homogeneity, uniform thickness, and infinite lateral extents of the aquifer. The Theis type-curve method (Theis method), developed by Theis and described by *Jacob* (1940), was developed from this work as a means to graphically infer hydrogeologic properties from pumping test data. *Cooper and Jacob* (1946) simplified this approach using an approximation to the Theis solution valid at late pumping times when a quasi-steady state regime is established (Jacob's method), eliminating the use of a Theis type curve. At quasi-steady state (also referred to as steady-shape), pressure gradients are steady, while pressures remain transient as second order terms become insignificant.

Wu et al. (2005) investigated the behavior of hydraulic parameters estimated using the Theis solution. Based on numerical experiments using multi-Gaussian transmissivity and storativity fields, the authors demonstrated that the interpreted transmissivity is time dependent at early times, with estimates from different locations converging (decreasing from larger values) towards a similar value at late times. They also demonstrate a time dependency for interpreted storativity, with values converging (increasing at some locations, decreasing at others) towards distinct values relatively quickly. This late-time convergent behavior corresponds with research by *Meier et al.* (1998) and *Sanchez-Vila et al.* (1999), who investigated the meaning of hydrogeologic parameter estimates obtained from Jacob's method numerically and analytically, respectively. *Straface et al.* (2007) evaluated hydrogeologic parameter inference methods using the Theis solution on a dataset from Montalto Uffugo Alto, Italy. Based on their results, they question the validity of hydrogeologic property inference based on the Theis solution. However, they do state that the Theis solution parameter estimates can be used as first estimates of hydrogeological parameters for a tomographic analysis.

We employ the Theis solution as our groundwater model in order to maintain a simple and efficient pressure-source identification approach (for a similar approach utilizing the Hantush solution in a time-series analysis framework, see *von Asmuth et al.* (2008)). In doing so, we recognize that the parameter estimates will be affected by the early-time pre-stabilization period, and cannot be considered as accurate estimates of hydrogeologic properties. Instead, these estimates can be considered as interpreted cross-hole parameters that characterize the hydraulic response at a monitoring location due to pumping a well, analogous to parameters that would be obtained from dedicated cross-hole pumping tests often used to characterize the hydrogeology of an aquifer. Here the term 'interpreted' follows the convention proposed by *Sanchez-Vila et al.* (2006).

This paper presents an approach to (1) fingerprint transient water-level variations to the pumping regime of individual water-supply wells and (2) estimate hydrogeologic characteristics using a computationally efficient analytical approach. Interpretation of the quantitative results from this approach can provide (1) indications of the large-scale structure inhibiting or promoting pressure propagation, (2) an evaluation of the information content in the calibration data (i.e. to what extent the observed water-level transients are characterizing pumping influences), and (3) guidance for the development of more complicated and computationally demanding models possessing the ability to explicitly consider heterogeneity.

As computational resources have become increasingly more powerful, the complexity and computational demand of models has proportionally increased. The concept of model parsimony is often lost or neglected in the quest to develop elaborate models that capture increasingly refined details of complexity. While complex models are required in certain applications, in other cases, a complex approach can mask fundamental insights that become obvious when the data are analyzed with models of minimal complexity. As noted by *Trinchero et al.* (2008), this situation can be encountered by fully or partially specifying porosity heterogeneity, where transport connectivity information is lost within the estimation of the distributed porosity parameter. Alternatively, *Trinchero et al.* (2008) demonstrate how transport point-to-point connectivity information can be captured within the estimate of a homogeneous porosity parameter. Similarly, fundamental insights into aquifer flow characteristics can be obtained considering homogeneous transmissivity and storativity parameters, which would be lost in distributed estimates of these parameters. The research presented here demonstrates an analysis of pumping and water-elevation records using a relatively simple model that provides fundamental insights into the aquifer pressure response and is a first step toward development of more complicated aquifer models that aim to characterize the groundwater flow complexity and aquifer heterogeneity utilizing the same data.

We demonstrate the proposed method using some of the pressure and water-supply pumping records from the regional aquifer at the Los Alamos National Laboratory (LANL) site located in north-central New Mexico, U.S.A.

Methodology

The goal of the analysis is to fingerprint transient water-level variations to the transients in the pumping regime of individual water-supply wells. To do this, we need a model that can simulate potential pumping influences at the monitoring wells (in time-series analysis, this is considered a transfer function (*Box et al.*, 1994)). A simple theoretically-based model that can be applied is the Theis solution, defined as

$$\hat{s}_p(t) = \frac{Q}{4\pi T} W(u) = \frac{Q}{4\pi T} W\left(\frac{r^2 S}{4Tt}\right) \quad (1)$$

where $\hat{s}_p(t)$ is the predicted drawdown due to pumping at time t since the pumping commenced, Q is the pumping rate, T is the transmissivity, $W(u)$ is the negative exponential integral ($\int_u^\infty e^{-y}/y\,dy$) referred to as the well function, $u = r^2S/4Tt$ is a dimensionless variable, r is radial distance from the pumping well, and S is the storativity. The assumption of homogeneity implicit in the Theis solution, discussed above, is apparent by the constant hydrogeologic parameters, T and S, in equation (1). Other assumptions implicit in the use of the Theis solution include (1) infinite aquifer extents, (2) fully penetrating wells, (3) confined conditions, and (4) two-dimensional flow. As discussed in the next section, while these assumptions are not strictly correct for our site application, arguments can be made for the use of the Theis solution here. It is important to note that more complicated analytical solutions accounting for partial well penetration, leakage effects, or three-dimensional flow could have been applied in our analyses as well, if the Theis solution had failed to identify the pumping influences adequately.

In order to include multiple pumping wells and variable rate pumping periods in the Theis solution, the principle of superposition is invoked as

$$\hat{s}_p(t) = \sum_{i=1}^{N}\sum_{j=1}^{M_i} \frac{Q_{i,j} - Q_{i,j-1}}{4\pi T_i} W\left(\frac{r_i^2 S_i}{4T_i(t - t_{Q_{i,j}})}\right) \tag{2}$$

where N is the number of pumping wells (sources), M_i is the number of pumping periods (i.e. the number of pumping rate changes) for pumping well i, $Q_{i,j}$ is the pumping rate of the ith well during the jth pumping period, r_i is the distance to the ith well from the observation point, and $t_{Q_{i,j}}$ is the time when the pumping rate changed at the ith well to the jth pumping period. The drawdown calculated by equation (2) represents the cumulative influence of the N pumping wells at a monitoring location.

Note that T_i and S_i are cross-hole parameters that characterize the influence of the ith pumping well at the observation location, conceptually similar to parameters that would be estimated from dedicated cross-hole pumping test analysis using the Theis method. As the significance of these parameters is limited by the assumptions of the Theis solution, we consider them interpreted parameters, and should not be confused with effective parameters (i.e. associated with ensemble averages of state variables) or equivalent parameters (i.e. associated with spatial averages of state variables) (*Sanchez-Vila et al.*, 2006).

In order to account for a temporal trend, which was found to be necessary in some cases in this research (monitoring wells R-11 and R-28), we include an additional drawdown term $\hat{s}_t(t)$ as

$$\hat{s}_t(t) = (t - t_o) * m \tag{3}$$

where t_o is the time at the beginning of the considered pumping record and m is the linear slope parameter defining the temporal trend of the water level not attributable to pumping. Linear and exponential temporal trends were evaluated here (analysis not presented) indicating that a linear trend is more plausible. While the temporal trend may be more complicated in reality, the linear trend is assumed to be sufficient for the pumping influence identification presented here without the risk of over-calibrating the model with more complicated functions describing the trend.

As the calibration targets are water elevations as opposed to drawdowns, we define the predicted water elevation $\hat{h}(t)$ at time t as

$$\hat{h}(t) = \hat{h}_o - \hat{s}_p(t) - \hat{s}_t(t) \tag{4}$$

where $\hat{h}_o = \hat{h}(0)$ (i.e. the simulated head at t_o) and is defined as the initial predicted water elevation at the observation well at the time the pumping begins. In order to account for pumping prior to the initiation of water-level monitoring, we include prior pumping records in the model. It is important to note that h_o is not the first water level observed at the commencement of water-level monitoring at the well. It is a computational parameter that reflects the simulated water level at the beginning of the water-supply pumping record (>2 months prior to the commencement of water-level monitoring; see Site Data section for details on monitoring and pumping record dates) which provides an optimal matching of the observed water levels. Additional analyses, not presented here, indicated that the inclusion of earlier pumping records had negligible impact on the identification results.

Model calibration is performed using a Levenberg-Marquardt approach (*Levenberg*, 1944; *Marquardt*, 1963) where the objective function is defined as

$$\mathbf{\Phi}(\theta) = \sum_{i=1}^{n} [h(t_i) - \hat{h}(t_i)]^2 \quad (5)$$

where θ contains the interpreted cross-hole parameters of T_i and S_i associated with each pumping well and $\hat{h}_o$ associated with the monitoring location of interest, and n is the number of head observations, $h(t_i)$, included as calibration targets, where i is an observation time index.

The simulation of the drawdowns is performed using the *WELLS* code (available for download at *Vesselinov* (2009); example files and user instructions are provided) which implements equation (4). The calibration is performed using *PEST* (*Doherty*, 2004).

Site Data

The regional aquifer beneath the LANL site is a complex stratified hydrogeologic structure which includes unconfined zones (under phreatic conditions near the regional water table) and confined zones (the deeper zones) (*Vesselinov*, 2004a,b). The aquifer is composed of volcanic fields consisting of fractured basalts and dacites that overlie and interfinger basin-fill sedimentary rocks (*Broxton and Vaniman*, 2005). At the regional scale, groundwater flow occurs in both fractured rock and alluvial sediments. However, at the scale of the study area (Figure 1) the groundwater flow is predominantly in sedimentary rocks. The three monitoring wells considered in this analysis are screened near the top of the aquifer with an average screen length of 11 meters. The water-supply wells partially penetrate the regional aquifer with screens that begin near the top of the aquifer, but penetrate deeper with an average screen length of 464 meters. Nevertheless, field tests demonstrate that most of the groundwater supply is produced from a relatively narrow section of the regional aquifer that is about 200-300 m below the regional water table (*Los Alamos National Laboratory*, 2008).

Due to concerns related to the migration of potential LANL-derived contaminants in the subsurface, a complex monitoring network is established in the regional aquifer beneath LANL. The network includes 92 regional monitoring wells with a total of 336 monitoring screens (*Allen and Koch*, 2008). At each screen, water-level fluctuations are automatically monitored using pressure transducers. In addition, water samples are collected for geochemical analysis. The aquifer beneath LANL is an important source of water for LANL and neighboring municipalities. There are 7 water-supply wells in close vicinity to the study area; 18 more water-supply wells are located nearby. The ultimate goal is to incorporate all these data in the development and calibration of the regional aquifer model. Here we analyze only a subset of the data from water-supply and monitoring wells, limiting our analysis to an area of current interest at the LANL site. While other pumping wells do exist on or near the LANL site, they are located at a sufficient distance that their influence is not observed at the monitoring wells evaluated here. The pressure and water-supply pumping records considered here are collected from 3 monitoring wells (R-11, R-15 and R-28) and 7 water-supply wells (PM-1, PM-2, PM-3, PM-4, PM-5, O-1, and O-4) located within the LANL site. Figure 1 displays a map of the spatial location of the wells and Table 1 tabulates the distances between monitoring and water-supply well pairs. Figure 2 presents the pressure and production records for the monitoring wells and water-supply wells, respectively.

Implicit in the use of the Theis solution is that the groundwater flow is two-dimensional. We assume that this is a justifiable assumption here given the small magnitude of observed drawdowns (less than 2 m at the monitoring wells and less than 20 m at the water-supply wells), the relatively long distances between supply and monitoring wells (more than 1 km; Table 1) compared to the effective aquifer thickness (about 200-300 m). The water-supply wells are screened in the deep aquifer zones that are predominantly under confined conditions. The three observation wells are screened in the shallow aquifer zones, near the regional water-table. Therefore, the groundwater flow in the zones between the pumping and observation wells is expected to be predominantly under confined conditions. Even if there are some characteristics of unconfined flow, the small magnitude of the drawdowns compared to the aquifer thickness justifies the use of Theis equation in this case. Future analyses will address the three-dimensionality of the groundwater flow and complex hydrostratigraphy of this aquifer.

Some of the groundwater pumped at the water-supply wells is derived from aquifer storage. However, due to seasonality of the water demands, there is substantial recovery in the low pumping periods (typically in January-February). When the water-supply wells are not used for significant periods of time, water-levels at the pumping wells recover to levels close to pre-pumping levels (*Koch and Schmeer*, 2009). The water-supply wells also capture some of the ambient flow that occurs in the regional aquifer between the zone of mountain-front recharge (approximately due west from the study area) and the zone of regional basin discharge (approximately due southeast of the study area) (*Vesselinov*, 2004b). The pressure fluctuations at the monitoring wells due to pumping are superposed on the ambient groundwater flow between these regional boundaries. The pressure fluctuations are not expected to be influenced by boundary effects due to aquifer properties and separation distances between the wells (pumping and monitoring) and the recharge/discharge zones (on the order of several kilometers) (*Vesselinov*, 2004b). However, changes in the recharge and discharge conditions at these regional boundaries may be causing the observed long-term decline of the water-levels. Such a decline of the water-levels has been observed at monitoring wells that are far from pumping wells (*Koch and Schmeer*, 2009). As a result, the pumping influences are superimposed on the ambient flow structure.

The water-level observation data considered here span nearly five years, commencing on or shortly after the date of installation of pressure transducers (May 4, 2005 for R-11; December 23, 2004 for R-15; February 14, 2005 for R-28), including records up to October 31, 2009. The barometric pressure fluctuations are removed using constant coefficient methods with 100% barometric efficiency (*LANL*, 2008) for all monitoring wells. Although the pressure transducers collect observations every 15 minutes, this dataset is reduced to single daily observations by using the earliest recorded measurement for each day. A single daily measurement is used as opposed to a daily average as barometric corrections are more complicated for average values, especially when data are missing. Some daily observations have been excluded due to equipment failure. The barometric-corrected water levels fluctuate over the five year period approximately 1 meter for R-11 (1642 daily records), 2 meters for R-15 (1774 daily records), and 1 meter for R-28 (1220 daily records). Seasonal trends are apparent in the water level data showing a general increase in the rate of decline during the summer months and recovery during the winter. The seasonal variations correlate well with seasonal variation in water-supply pumping, and, given the thickness of the unsaturated zone, are not expected to be caused by seasonal precipitation and/or evaporation. Similarities are evident for water-level observations at R-11 and R-28 providing an initial indication that there is a region of similar hydrogeological properties around these two monitoring wells.

Considered pumping records for all pumping wells begin on October 8, 2004 and terminate on October 31, 2009. The pumping record precedes the water-level calibration data to include any pumping influences before the water-level data collection commenced. As mentioned above, inclusion of earlier pumping records did not significantly alter the pumping influence identification results. The number of pumping-rate changes for each well are: PM-1 – 3147; PM-2 – 1727; PM-3 – 2001; PM-4 – 689; PM-5 – 2805; O-1 – 41; and O-4 – 3318. Daily volumetric production values are converted to time intervals of pumping using the constant pumping rates for each well for use in the forward models.

Drawing correlations between pressure and pumping transients from a visual comparison of the plots in Figure 2 is difficult, except perhaps an apparent influence of PM-4 pumping on monitoring well R-15 (indicating that point-to-point flow connectivity is likely an important characteristic of the aquifer). Therefore it is essential to fingerprint the water level transients to the pumping records in order to determine the hydraulic connections within the aquifer.

In the applied computational framework, forward model run times for predicting water elevations at R-11, R-15, and R-28 are approximately 9 seconds on a 3.0 GHz Intel processor. Inversions initiated with uniform initial parameter values require approximately 600 model runs and, using a single processor, are performed for approximately 1 hour and 40 minutes.

Results and Discussion

The inversions for each monitoring well are performed separately so that the calibration can focus on identifying the pressure influences in the water-level transients for an individual monitoring location. Simultaneous inversion of the calibration data from all the monitoring wells is also possible, and would be the desired approach for the estimation of aquifer heterogeneity and effective aquifer properties; this will be the subject of future analyses. However, such analyses are expected to rely on more complicated methods for simulation of the pumping responses of the aquifer.

Figures 3, 4, and 5 present the decomposed drawdown contributions from the water-supply wells for monitoring wells R-11, R-15, and R-28, respectively. The associated water-supply pumping record is plotted along with each drawdown contribution to illustrate the calibrated pressure influence at the monitoring wells attributed to each water-supply well. The observed and simulated pressure transients for the associated monitoring well are plotted along the top of Figures 3, 4, and 5 for reference. Pumping wells that are not included in the figures were assigned values by the calibration algorithm which resulted in negligible drawdown. In other words, these wells were effectively "shut off" by the calibration as parameter values resulting in drawdown that improved the matching of observations could not be identified for these wells. To further ensure that the pumping influences of these wells could not be fingerprinted at the monitoring location, additional calibrations were performed focusing on each "shut off" well individually using sets of alternative initial guesses for the optimized parameters. In all cases, the calibration adjusted the parameters of these wells to values resulting in negligible drawdown again (details of these analyses are not presented here), providing further indication that the calibration is unable to fingerprint the pressure influence of these pumping wells at the respective monitoring well.

The model identifies a temporal trend of groundwater decline for wells R-11 and R-28 (0.075m/a and 0.078m/a, respectively), but not for R-15 (i.e. the calibration assigned a negligible value to the slope parameter m in equation (3) for R-15; $m < 10^{-6}$m/a). The declining trend is needed in addition to the drawdown contributions from the individual supply wells for R-11 and R-28 to adequately predict the overall drawdown. Note that R-11 and R-28 water levels appear to be impacted by similar trends. The cause of this temporal trend has not been identified, but it may be related to factors not directly related to the water-supply pumping (e.g. reduction in aquifer recharge). The reason that a similar trend is not identified at R-15 is not well understood at the moment, but may be due to the differences in the local hydrogeologic conditions at these wells.

It is apparent that the inversions identify, or fingerprint, the pumping records from PM-2, PM-3, and PM-4 as influencing the water-level observations at each of the monitoring wells, while PM-5 pumping is identified to influence R-15. This analysis also suggests that there is a lack of point-to-point flow connectivity between O-4 and the monitoring wells. This is somewhat surprising considering the well locations and the substantial water production at O-4. It appears that similar hydrogeologic conditions may exist to the east of PM-

3, given the lack of pressure influence attributed to PM-1. The aquifer features causing these differences in flow connectivity will be investigated further with more complex models capable of explicitly considering spatial aquifer heterogeneity and three-dimensionality of groundwater flow.

Autocorrelation plots of the residuals are presented in Figure 6. The difference in the lag length evaluated for each monitoring well reflects the difference in continuous record lengths. It is apparent that the residuals are autocorrelated at some lags, indicating influences which cannot be attributed to pumping or linear temporal trends. Since the pumping records are the only reliable quantitative indications of stresses applied to the aquifer, we do not consider these residual autocorrelations easily reducible. Residuals between observed and model predicted water-levels might also be caused by systematic errors in the calibration data set; for example, barometric pressure effects might not have been entirely removed from the calibration data set. It should also be noted that the existence of these autocorrelations in residuals of relatively small magnitude (on the order of centimeters) does not indicate an inability to identify the pumping influences on the water-level transients.

Table 2 contains interpreted cross-hole transmissivity and storativity parameters obtained from the calibrations presented in Figures 3, 4, and 5. The linear 95% confidence intervals for the log (base 10) transformed values are presented. These confidence intervals serve as an approximation based on an assumption that the applied model is linear and the residuals are unbiased and Gaussian (*Doherty*, 2004). As these assumptions are not valid here, the actual nonlinear 95% confidence intervals are expected to be slightly larger. As discussed previously, these parameters characterize the hydraulic response between pumping and monitoring wells within the context of the Theis solution, conceptually similar to estimates that would be obtained by analysis of dedicated cross-hole pumping tests using the Theis type curve approach. Unrealistic values for storativity are expected, and should not be considered as estimates of actual storativity. These interpreted storativities may provide indications of point-to-point flow connectivity (i.e. large/small S indicates low/high flow connectivity) (*Meier et al.*, 1998; *Sanchez-Vila et al.*, 1999; *Trinchero et al.*, 2008), however, drawdown calculations performed outside of the Cooper-Jacob constraint are expected to cause additional variations in these values (*Wu et al.*, 2005).

Due to nonlinear effects not captured in the Theis solution (unconfined flow, leakance, aquifer heterogeneity), different values for these parameters may be obtained if pumping records with a substantially different regime are evaluated (e.g. higher or lower pumping rates, long recovery periods, etc.). For example, we performed analyses similar to those presented here, utilizing shorter data record periods. Using approximately two- and three-year data records produced different estimates for the parameters (within three-quarters of an order of magnitude difference for interpreted transmissivities); however, the identification of the pumping wells influencing a monitoring location remained the same despite the length of the record evaluated. Additional analyses will be performed in the future to evaluate the impact of data record length on the estimation of interpreted parameters.

Conclusions

The approach described in this paper allows the identification of pressure-influence sources at a monitoring location utilizing existing long-term pumping and water-elevation records. This type of dataset is often available from monitoring-well networks established near municipal water-supply well fields. The approach provides fingerprinting of pumping influences in pressure transients to identify drawdown contributions from individual water-supply wells and information about the zone of influence of individual pumping wells. The presented analysis is computationally efficient due to the utilization of a simple analytical model, which facilitates the processing of large amounts of data associated with long-term records. The same analysis will be computationally very demanding and potentially not effective using more complex models representing details of the aquifer heterogeneity. Utilization of such datasets provides several advantages over conducting dedicated cross-hole pumping tests, including the ability to consider long-term records with multiple variable pumping regimes. Interpretation of the results can provide (1) indications of large-scale hydrogeologic structures within the aquifer inhibiting or promoting pressure propagation and (2) guidance for the development of more complicated models requiring detailed knowledge of aquifer heterogeneity.

Utilizing this approach on a dataset from the LANL site has indicated that (1) relatively small magnitude water-level transients do not preclude our ability to identify the pumping wells influencing water levels at a monitoring location and (2) water-levels at some of the wells exhibit a declining temporal trend that cannot be directly attributed to any of the pumping wells. Future work will include more complicated analytical solutions that can account for partial penetration of pumping and observation wells, aquifer anisotropy, three-dimensional flow, and leakage from overlying strata. Future work will also include data from additional monitoring wells, coupled inversions (i.e. inversions including data from multiple monitoring wells simultaneously), spatial analysis of aquifer heterogeneity utilizing numerical models based on tomographic techniques, and characterization of the three-dimensional structure of aquifer heterogeneity and groundwater flow.

The results also provide guidance for development of more complicated numerical models of the site. Our analyses suggest that numerical models characterizing the aquifer heterogeneity will benefit substantially if the long-term pumping and water-level records are incorporated in the calibration process. The spatial representation of the aquifer heterogeneity should be (1) capable to represent the identified large-scale aquifer structures and (2) with resolution sufficient to represent the differences in the water-level transients at R-15 and R-11/R-28. The model should also be capable of accounting for water-level declines that may not be directly associated with pumping transients. The results show that it is critical to account for the three-dimensional structure of the groundwater flow.

Acknowledgments

The research was funded through various projects supported by the Environmental Programs Division at the Los Alamos National Laboratory. The authors are thankful for the valuable suggestions and comments provided by Kay Birdsell, Jos von Asmuth, Roger D. Congdon, and two anonymous reviewers on draft versions of this paper. The authors are also grateful for constructive comments provided by members of the first author's Ph.D. advisory committee (Bruce Thomson, Gary Weissmann, and John Stormont).

References

Alcolea, A., J. Carrera, and A. Medina (2006), Pilot points method incorporating prior information for solving the groundwater flow inverse problem, *Advances in Water Resources*, *29*, 1678–1689.

Allen, S., and R. Koch (2008), Groundwater level status report for fiscal year 2007, *Progress Report LA-14358-PR*, Los Alamos National Laboratory, available at http://library.lanl.gov/cgi-bin/getfile?LA-14358-PR.pdf.

Barnett, D., J. Rieger, and E. Thornton (2003), Results of tritium tracking and groundwater monitoring at the Hanford Site 200 area state-approved land disposal site–fiscal year 2003, *Tech. Rep. PNNL-14449*, Pacific Northwest National Laboratory.

Beven, K. (2000), Uniqueness of place and process representations in hydrological modelling, *Hydrology and Earth Systems Sciences*, *4*(2), 203–213.

Beven, K. (2006), A manifesto for the equifinality thesis, *Journal of Hydrology*, *320*, 18–36.

Box, G. E., G. M. Jenkins, and G. C. Reinsel (1994), *Time Series Analysis: Forcasting and Control*, 3 ed., Prentice Hall.

Broxton, D., and D. Vaniman (2005), Geologic framework of a groundwater system on the margin of a rift basin, Pajarito Plateau, north-central New Mexico, *Vadose Zone Journal*, *4*, 522–550, doi:10.2136/vzj2004.0073.

Carrera, J., A. Alcolea, A. Medina, J. Hidalgo, and L. Slooten (2005), Inverse problem in hydrogeology, *Hydrogeology Journal*, *13*, 206–222.

Certes, C., and G. de Marsily (1991), Application of the pilot point method to the identification of aquifer transmissivities, *Advances in Water Resources*, *14*(5), 284–300.

Cooper, H., and C. Jacob (1946), A generalized graphical method for evaluating formation constants and summarizing well-field history, *Eos Trans. AGU*, *27*(4), 526–534.

Doherty, J. (2004), *PEST Model-Independent Parameter Estimation*, Watermark Numerical Computing, Corinda, Australia.

Freeze, R., and J. Cherry (1979), *Groundwater*, Prentice Hall, Englewood Cliffs, NJ.

Gómez-Hernández, J., A. Sahuquillo, and J. Capilla (1997), Stochastic simulation of transmissivity fields conditional to both trasmissivity and piezometric data. 1. theory, *Journal of Hydrology*, *204*(1-4), 162–174.

Grayson, R., I. Moore, and T. McMahon (1992), Physically based hydrologic modeling 2. is the concept realistic?, *Water Resources Research*, *26*(10), 2659–2666.

Gross, L. (2007), Use of geostatistics to evaluate the monitoring well network of a TCE plume, *International Journal of Environment and Pollution*, *29*(4), 370–382.

Harp, D., Z. Dai, A. Wolfsberg, J. Vrugt, B. Robinson, and V. Vesselinov (2008), Aquifer structure identification using stochastic inversion, *Geophysical Research Letters*, L08404, doi:10.1029/2008GL033585, l08404, doi:10.1029/2008GL033585.

Hendricks Franssen, H., and W. Kinzelbach (2008), Real-time groundwater flow modeling with the Ensemble Kalman Filter: Joint estimation of states and parameters and the filter inbreeding problem, *Water Resources Research*, *44*, W09408, doi:10.1029/2007WR006505.

Hix, G. (2007), Ground-water monitoring in the Tucson Basin, Pima County, Arizona, *Ground Water Monitoring and Remediation*, *1*, 36–38.

Jacob, C. (1940), On the flow of water in an elastic artesian aquifer, *Trans. Amer. Geophys. Union*, *21*, 574–586.

Koch, R., and S. Schmeer (2009), Groundwater level status report for 2008, Los Alamos National Laboratory, *Tech. Rep. LA-14397-PR*, Los Alamos National Laboratory, available at http://www.ees.lanl.gov/staff/monty/reports/.

LANL (2008), Fate and transport investigations update for chromium contamination from Sandia Canyon, *Tech. rep.*, Environmental Programs Directorate, Los Alamos National Laboratory, Los Alamos, New Mexico, LA-UR-08-4702.

Levenberg, K. (1944), A method for the solution of certain nonlinear problems in least squares, *Q. Appl. Math.*, *2*, 164–168.

Los Alamos National Laboratory (2008), Pajarito canyon investigation report, *Tech. Rep. LA-UR-085852*, Los Alamos National Laboratory.

Marquardt, D. (1963), An algorithm for least-squares estimation of nonlinear parameters, *J. Soc. Ind. Appl. Math.*, *11*, 431–441.

Mason, J., S. Sebree, and T. Quinn (2005), Monitoring-well network and sampling design for ground-water quality, Wind River Indian Reservation, Wyoming, *Scientific Investigations Report 2005-5027*, USGS.

Meier, P., J. Carrera, and X. Sanchez-Vila (1998), An evaluation of Jacob's method for the interpretation of pumping tests in heterogeneous formations, *Water Resources Research*, *34*(5), 1011–1025.

Neuman, S. (1987), Stochastic continuum representations of fractured rock permeability as an alternative to the REV and fracture network concepts, in *Rock Mechanics: Proceedings of the 28th U.S. Symposium*, edited by I.W. Farmer et al., pp. 533–561, Springfield, Vt.

Sanchez-Vila, X., P. Meier, and J. Carrera (1999), Pumping tests in heterogeneous aquifers: An analytical study of what can be obtained from their interpretation using Jacob's method, *Water Resources Research*, *35*(4), 943–952.

Sanchez-Vila, X., A. Guadagnini, and J. Carrera (2006), Representative hydraulic conductivities in saturated groundwater flow, *Reviews of Geophysics*, *44*, RG2=3002, doi:8755-1209/06/2005RG000169.

Straface, S., T.-C. J. Yeh, J. Zhu, S. Troisi, and C. Lee (2007), Sequential aquifer tests at a well field, Montalto, Uffugo Scalo, Italy, *Water Resources Research*, *43*, W07432, doi:10.1029/2006WR005287.

Theis, C. (1935), The relation between the lowering of the piezometric surface and the rate and duration of discharge of a well using ground-water storage, *Eos Trans. AGU*, *16*, 519–524.

Trinchero, P., X. Sánchez-Vila, and D. Feràndez-Garcia (2008), Point-to-point connectivity, an abstract concept or a key issue for risk assessment studies?, *Advances in Water Resources*, *31*, 1742–1753.

Vesselinov, V. (2004a), An alternative conceptual model of groundwater flow and transport in saturated zone beneath the pajarito plateau, *Tech. Rep. LA-UR-05-6741*, Los Alamos National Laboratory.

Vesselinov, V. (2004b), Logical framework for development and discrimination of alternative conceptual models of saturated groundwater flow beneath the pajarito plateau, *Tech. Rep. LA-UR-05-6876*, Los Alamos National Laboratory.

Vesselinov, V. (2009), http://www.ees.lanl.gov/staff/monty/codes/wells.

Vesselinov, V., S. Neuman, and W. Illman (2001), Three-dimensional numerical inversion of pneumatic cross-hole tests in unsaturated fractured tuff 2. equivalent parameters, high-resolution stochastic imaging and scale effects, *Water Resources Research*, *37*(12), 3019–3041.

von Asmuth, J. R., K. Maas, and J. Petersen (2008), Modeling time series of ground water head fluctuations subjected to multiple stresses, *Ground Water*, *46*(1), 30–40.

Vrugt, J., C. Dirks, H. Gupta, W. Bouten, and J. Verstraten (2005), Improved treatment of uncertainty in hydrologic modeling: Combining the strengths of global optimization and data assimilation, *Water Resources Research*, *41*, W01017, doi:10.1029/2004WR003059.

Wu, C.-M., T.-C. Yeh, J. Zhu, T. Lee, N. Hsu, C.-H. Chen, and A. Sancho (2005), Traditional analysis of aquifer tests: Comparing apples to oranges?, *Water Resources Research*, *41*, W09402, doi:10.1029/2004WR003717.

Yeh, T.-C. J., and C.-H. Lee (2007), Time to change the way we collect and analyze data for aquifer characterization, *Ground Water*, *45*(2), technical Commentary.

Tables

	PM-1	PM-2	PM-3	PM-4	PM-5	O-1	O-4
R-11	2399.8	2902.7	803.6	1929.9	2439.5	3007.2	1367.7
R-15	3787.7	2434.7	2252.2	1081.0	986.0	4460.3	1566.7
R-28	2666.7	2522.4	1154.3	1506.3	2103.8	3384.8	1500.2

Table 1: Distances between pumping and monitoring well pairs in meters, where the row headings indicate the monitoring wells and column headings indicate the pumping wells.

Hydrogeologic Property	Monitoring Well	Pumping well						
		PM-1	PM-2	PM-3	PM-4	PM-5	O-1	O-4
Interpreted	R-11	-	4.25 ± 0.09	3.41 ± 0.03	3.14 ± 0.02	-	-	-
transmissivity	R-15	-	3.55 ± 0.04	3.40 ± 0.05	2.96 ± 0.01	3.52 ± 0.06	-	-
$log_{10}[m^2/d]$	R-28	-	4.43 ± 0.14	3.50 ± 0.04	3.44 ± 0.02	-	-	-
	R-11	-	-1.69 ± 0.18	-0.25 ± 0.02	-1.06 ± 0.01	-	-	-
Interpreted		-	(0.020)	(0.562)	(0.087)	-	-	-
storativity	R-15	-	-2.09 ± 0.07	-1.41 ± 0.04	-1.66 ± 0.01	-1.07 ± 0.07	-	-
$log_{10}[-]$		-	(0.008)	(0.039)	(0.022)	(0.085)	-	-
([−])	R-28	-	-1.72 ± 0.34	-0.70 ± 0.03	-1.23 ± 0.02	-	-	-
		-	(0.019)	(0.200)	(0.058)	-	-	-

Table 2: Interpreted cross-hole parameters from model inversions. Log (base 10) transformed values and their associated linear 95% confidence interval are presented. Non-transformed storativities are presented in parenthesis for ease of interpretation. Dashes indicate interpreted parameters that the calibration assigned values resulting in negligible drawdown ($T > 10^6$ and $S > 0.03$), effectively eliminating the influence of the pumping well at the monitoring well. The linear slope parameters describing the temporal trend (not attributable to pumping) at R-11, R-15, and R-28 (not presented in the table) are -0.075 m/a, 0 m/a, and -0.078 m/a, respectively.

Figure Captions

Figure 1. Map of observation wells (circles) and water-supply wells (stars) included in the analysis.

Figure 2. Water elevations at monitoring wells and production records for water-supply wells.

Figure 3. Top plot: simulated (black) and observed (gray) water elevations for R-11 model inversion. Second plot: residuals between simulated and observed values. Bottom plots: predicted drawdown contributions (black lines) from individual pumping wells, plotted with their associated pumping record (gray bars), and temporal trend required to reproduce the total predicted drawdown at R-11.

Figure 4. Top plot: simulated (black) and observed (gray) water elevations for R-15 model inversion. Second plot: residuals between simulated and observed values. Bottom plots: predicted drawdown contributions (black lines) from individual pumping wells, plotted with their associated pumping record (gray bars), required to reproduce the total predicted drawdown at R-15.

Figure 5. Top plot: simulated (black) and observed (gray) water elevations for R-28 model inversion. Second plot: residuals between simulated and observed values. Bottom plots: predicted drawdown contributions (black lines) from individual pumping wells, plotted with their associated pumping record (gray bars), and temporal trend required to reproduce the total predicted drawdown at R-28.

Figure 6. Residual autocorrelations for the monitoring wells.

547 # Figures

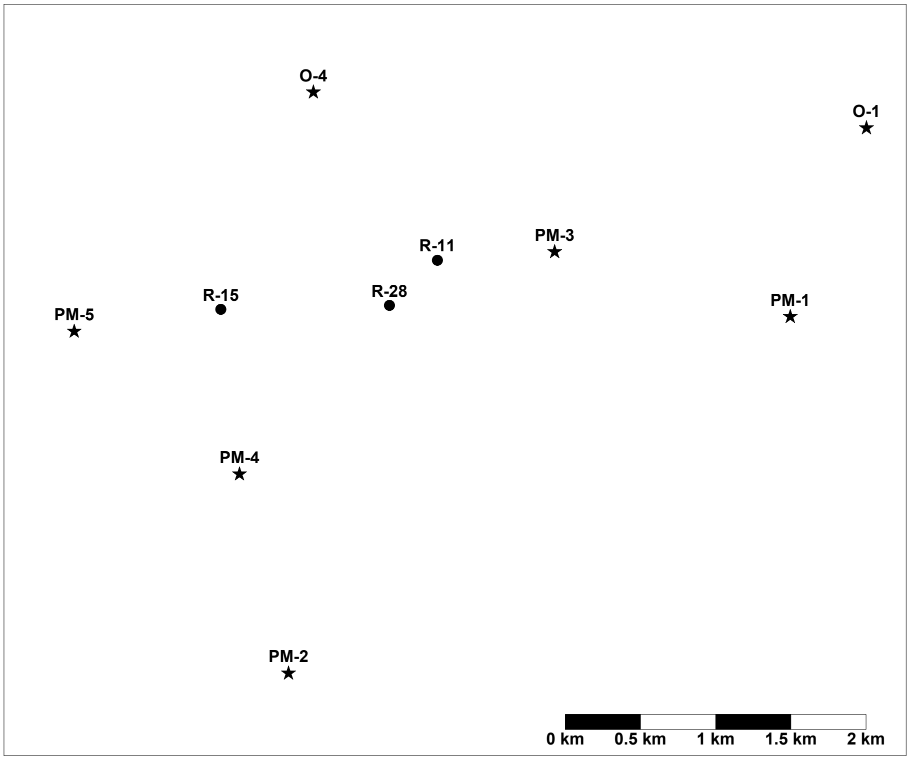

Figure 1: Map of observation wells (circles) and water-supply wells (stars) included in the analysis.

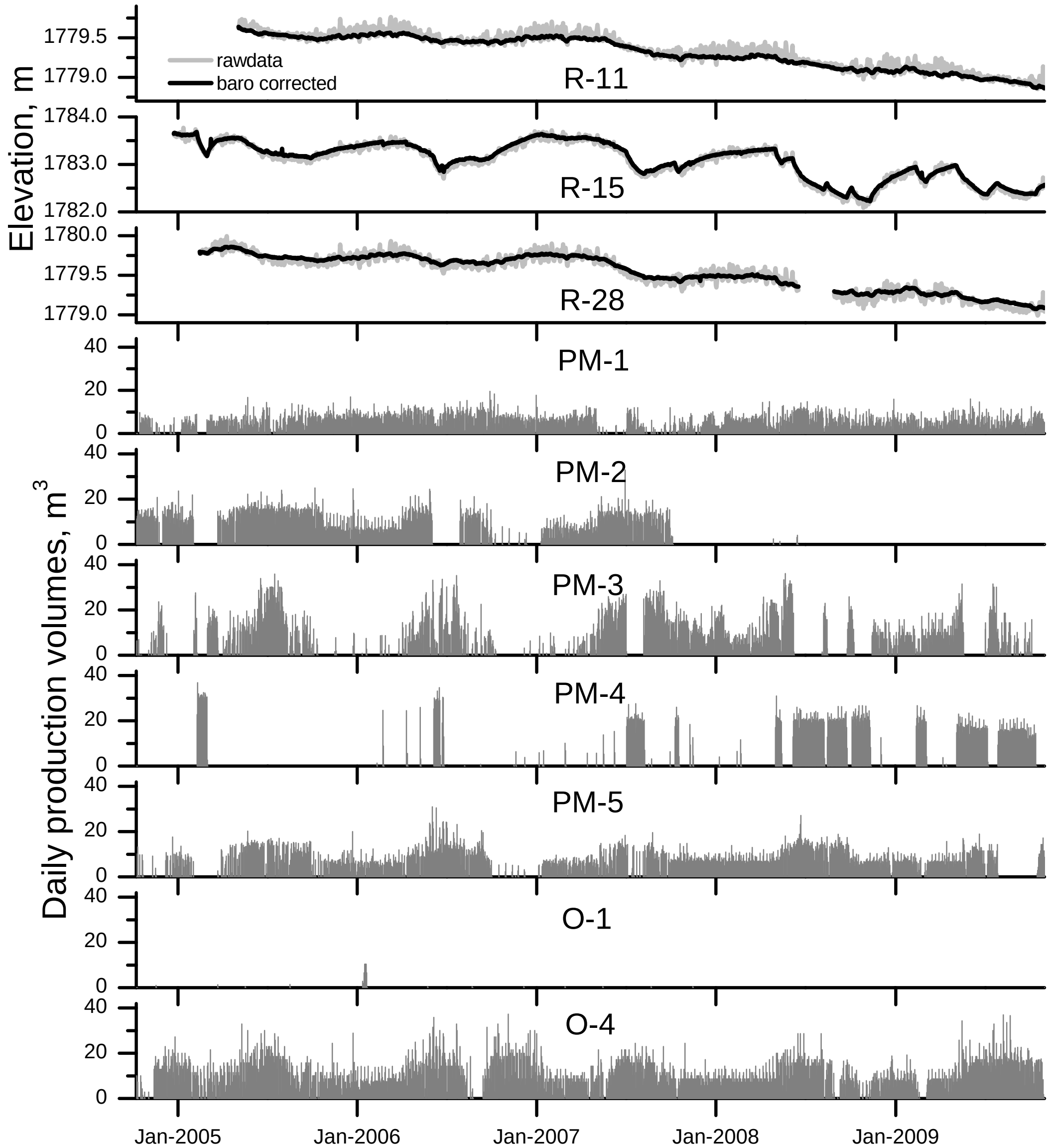

Figure 2: Water elevations at monitoring wells and production records for water-supply wells.

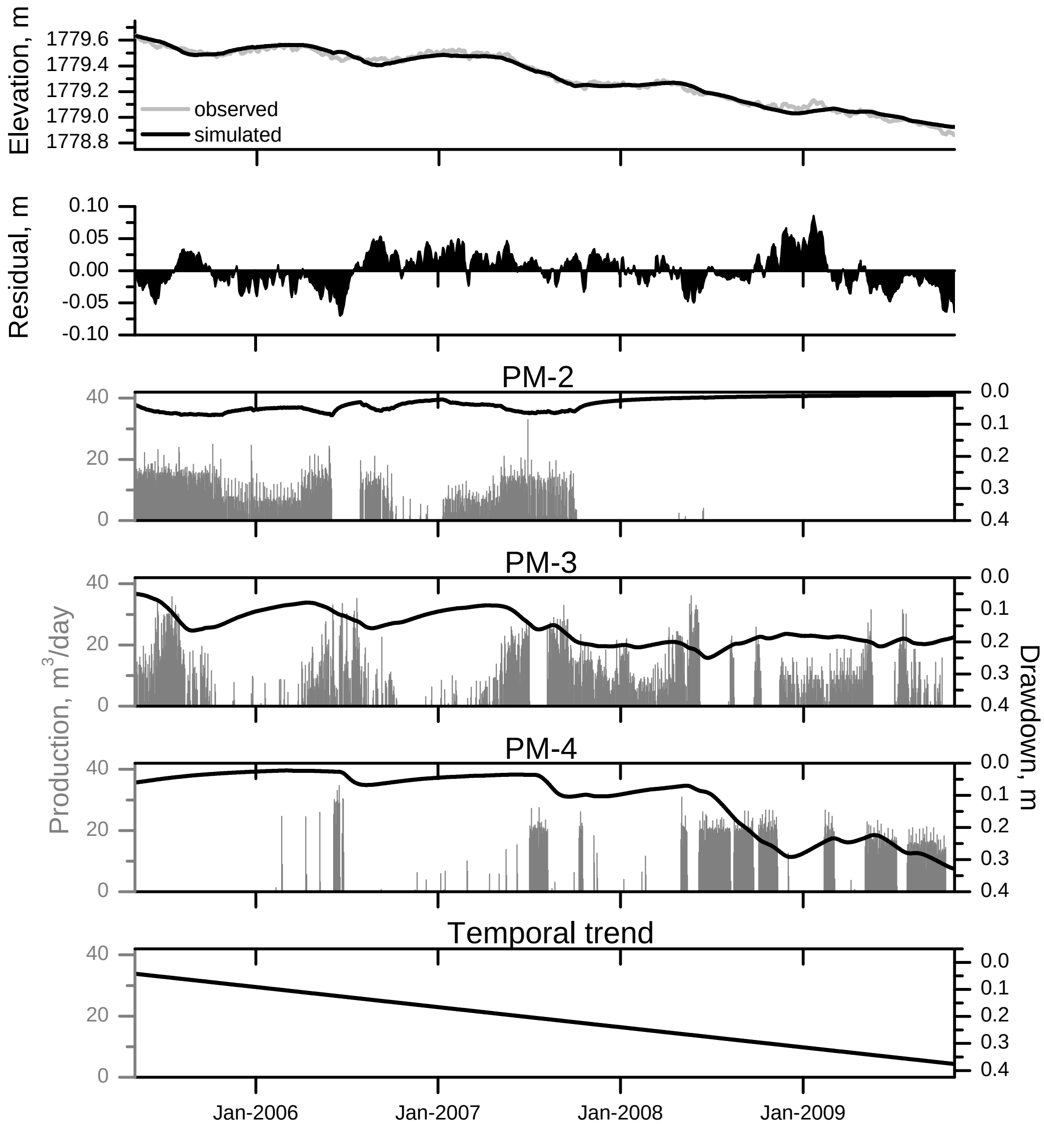

Figure 3: Top plot: simulated (black) and observed (gray) water elevations for R-11 model inversion. Second plot: residuals between simulated and observed values. Bottom plots: predicted drawdown contributions (black lines) from individual pumping wells, plotted with their associated pumping record (gray bars), and temporal trend required to reproduce the total predicted drawdown at R-11.

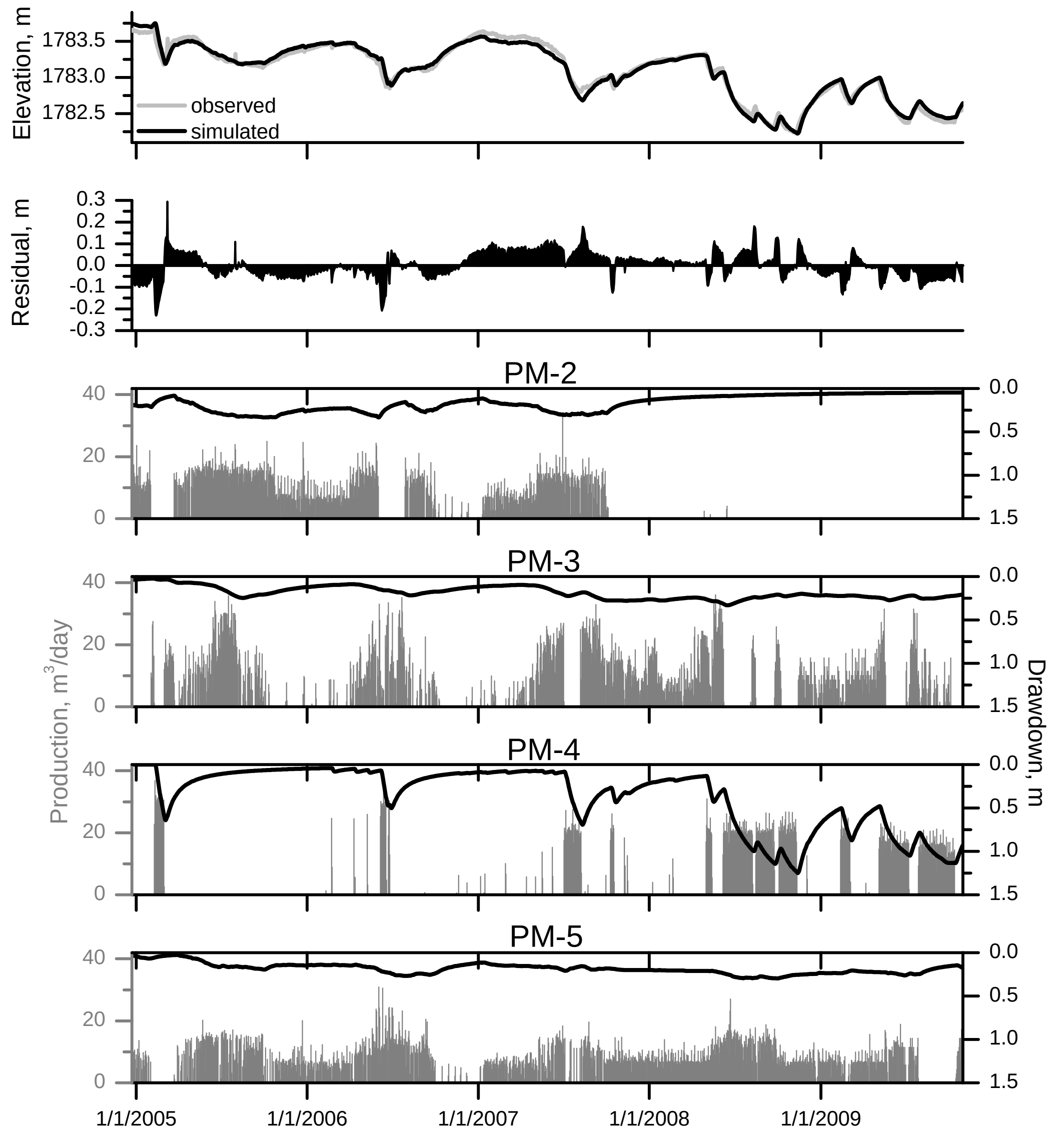

Figure 4: Top plot: simulated (black) and observed (gray) water elevations for R-15 model inversion. Second plot: residuals between simulated and observed values. Bottom plots: predicted drawdown contributions (black lines) from individual pumping wells, plotted with their associated pumping record (gray bars), required to reproduce the total predicted drawdown at R-15.

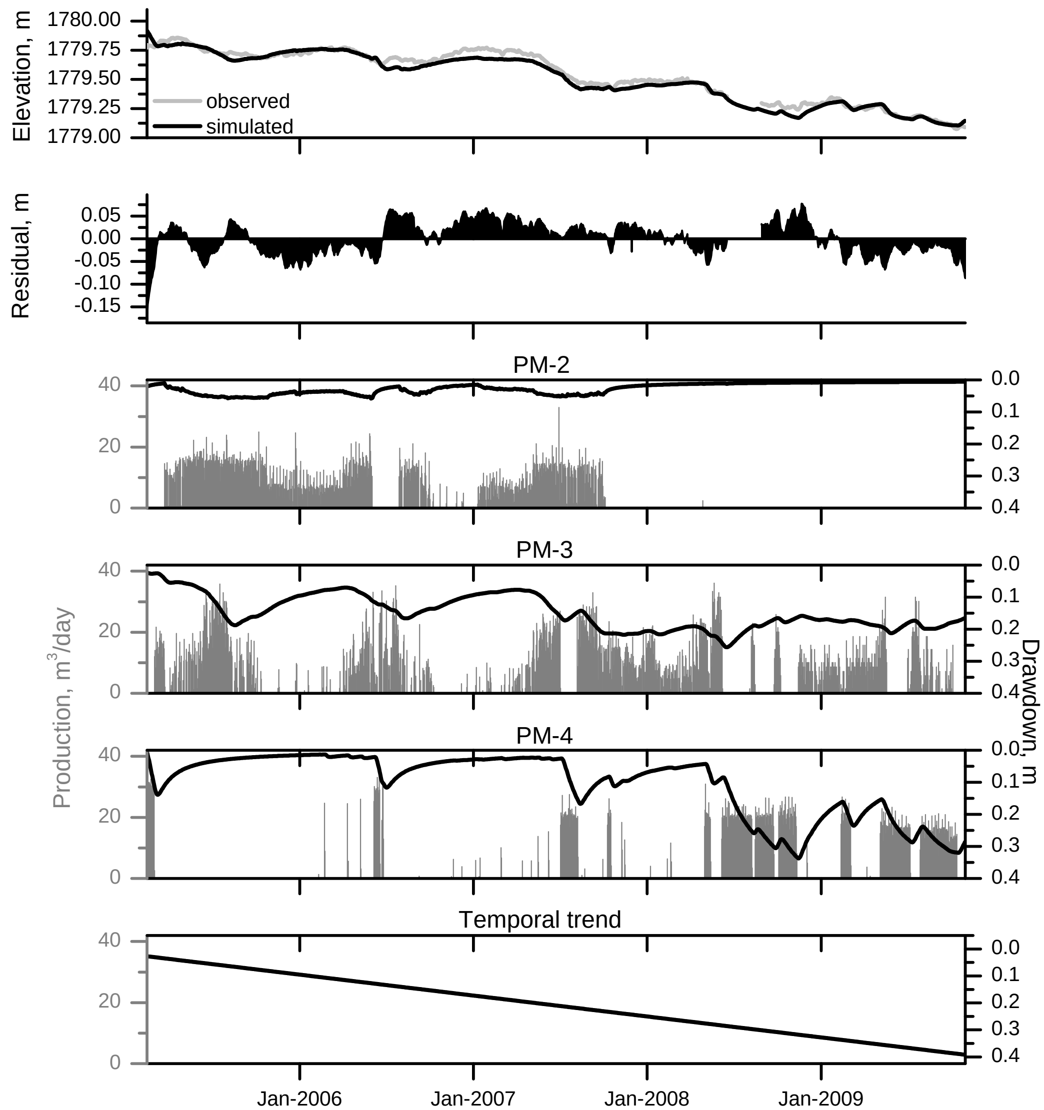

Figure 5: Top plot: simulated (black) and observed (gray) water elevations for R-28 model inversion. Second plot: residuals between simulated and observed values. Bottom plots: predicted drawdown contributions (black lines) from individual pumping wells, plotted with their associated pumping record (gray bars), and temporal trend required to reproduce the total predicted drawdown at R-28.

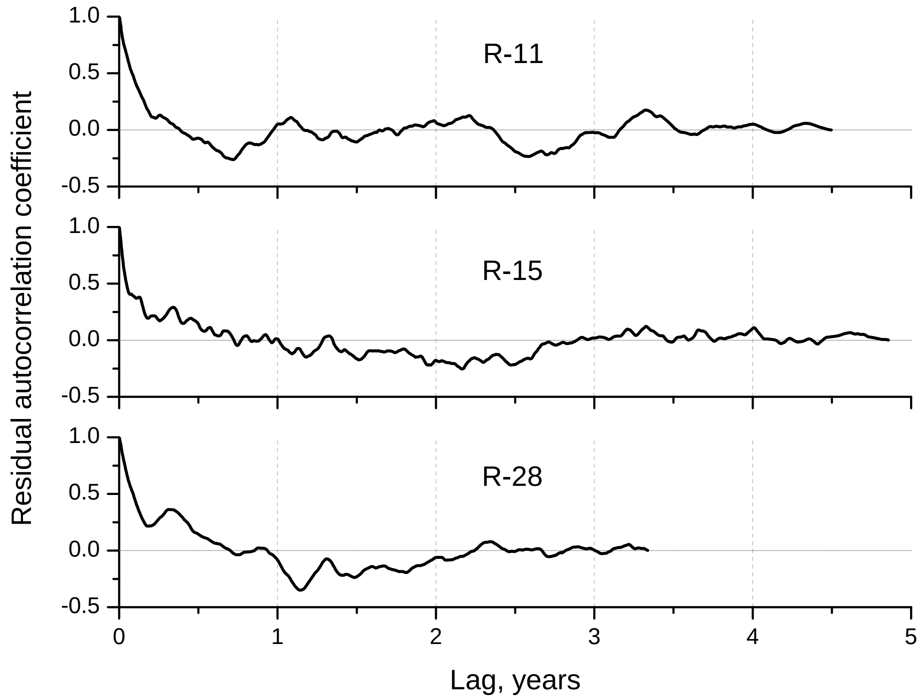

Figure 6: Residual autocorrelations for the monitoring wells.